


DOI: <https://doi.org/10.26628/simp.wtr.v98.1196.3-14>

Original Article

The Influence of Electron Beam Welding on the Microstructure and Mechanical Properties of AlMgSi (Cu) alloys

Sonia Boczekal ¹, Bartłomiej Płonka ², Joanna Hrabia-Wisnios ^{3,*}, Monika Mitka ⁴, Marek St. Węglowski ⁵, Śliwiński Piotr ⁶, Paweł Pogorzelski ⁷, Marcin Fiołka ⁸, Krzysztof Fiołka ⁹

¹ Łukasiewicz - Institute of Non-Ferrous Metals; Light Metals Centre, Pilsudskiego 19 Street, 32-050 Skawina, Poland; sonia.boczekal@imn.lukasiewicz.gov.pl (S.B.)

² Łukasiewicz - Institute of Non-Ferrous Metals; Light Metals Centre, Pilsudskiego 19 Street, 32-050 Skawina, Poland; barlomiej.plonka@imn.lukasiewicz.gov.pl (B.P.)

³ Łukasiewicz - Institute of Non-Ferrous Metals; Light Metals Centre, Pilsudskiego 19 Street, 32-050 Skawina, Poland; joanna.hrabia-wisnios@imn.lukasiewicz.gov.pl (J.H.)

⁴ Łukasiewicz - Institute of Non-Ferrous Metals; Light Metals Centre, Pilsudskiego 19 Street, Skawina, Poland; monika.mitka@imn.lukasiewicz.gov.pl (M.M.)

⁵ Ennecor Ltd., Wincentego Pola 27 Street, 44-100 Gliwice; marek.weglowski@ennecor.pl, (M.W.)

⁶ Łukasiewicz - Upper Silesian Institute of Technology, Welding Centre, Karola Miarki 12-14 Str., 44-100 Gliwice, Poland; piotr.sliwinski@git.lukasiewicz.gov.pl (P.S.)

⁷ Łukasiewicz - Upper Silesian Institute of Technology, Welding Centre, Karola Miarki 12-14 Str., 44-100 Gliwice, Poland; pawel.pogorzelski@git.lukasiewicz.gov.pl (P.P.)

⁸ Ennecor Ltd., Wincentego Pola 27 Street, 44-100 Gliwice; marcin.fiolka@ennecor.pl (M.F.)

⁹ Ennecor Ltd., Wincentego Pola 27 Street, 44-100 Gliwice; krzysztof.fiolka@ennecor.pl (K.F.)

* Correspondence: joanna.hrabia-wisnios@imn.lukasiewicz.gov.pl; Łukasiewicz - Institute of Non-Ferrous Metals; Light Metals Centre, Pilsudskiego 19 Street, 32-050 Skawina, Poland) (J.H.)

Received: 11.02.2026; Accepted: 14.03.2026; Published: 15.03.2026

Abstract: For many commonly used aluminium alloys, electron beam welding (EBW) is a very suitable welding process. In this study, the influence of EBW technological parameters on properties of AlSiMg(Cu) welded joints were discussed. SEM and EDS analysis studies were conducted to examine the effects of alloying elements as well as EBW parameters on the properties of welded joints. The conducted experiments revealed that the use of EB can produce welds with high quality. Porosity as well as cracks were not observed. The welding speed of 2000 mm/min have resulted in narrow width of welds for all alloys. In comparison with different alloys has experienced severe deterioration in mechanical properties due to softening in the fusion zone resulting from dissolution of the strengthening precipitates in the weld metal and HAZ, such deterioration is in the range of AlSiMg(Cu) 81-99% of base material. The results have shown that, the microhardness increase in HAZ for all welded joints up to 116 HV1 (alloy 3B), and strength for the same alloy up to 275 MPa (base material 277 MPa). Thus, the max joint efficiency is 99%. However, the bend tests indicated that cracks up 3.5 mm occurred.

Keywords: 6xxx; electron beam welding; joining; aluminium alloys

Introduction

Depending on the required mechanical properties, corrosion resistance and application of aluminium alloys a different alloying element can be applied. Aluminium is the most alloyed with copper, zinc, magnesium, silicon, manganese and lithium. Small additions of chromium, titanium, zirconium, lead, bismuth and nickel are also used, and iron is invariably present in small quantities. There are over 300 wrought aluminium alloys with 50 in common use. Owing to their good strength, formability and corrosion properties, the Al-Mg-Si(Cu) alloys are important for the automotive industry. Copper as an alloying element allows to increase strength, hardness, fatigue, creep resistance and machinability in an aluminum-silicon alloy. Strength and ductility depend on how copper is distributed in the alloy. Copper is found dissolved in the dendrite matrix or as aluminium-copper rich phases. Aluminium alloys with dissolved copper in the matrix shows the most increase of strength and retains ductility. Continuous network of copper at the grain boundaries increases the strength to appreciable levels but the ductility decreases [1]. To increase the content of copper in the alloy a higher hardness is achieved, and porosity formation increases. Shabestari

et al. [2] revealed that, the Al–7% Si–0.35% Mg alloy containing 1.5 wt.% copper has the optimum mechanical properties compared to the alloys having lower or higher copper content than 1.5 wt.%. Moreover, it should be noted that alloy density increases with copper content, and the highest densities are obtained in graphite mold. Simultaneously, the porosity volume percentage increases with copper content in different solidification conditions. Li et al. [3] have indicated that the tensile strength (UTS) increases with Cu content in the Al–Si–Mg–Cu alloys. A significant improvement of the tensile strength has been achieved in the alloy with addition of 3.0 wt.% Cu. The 3.0 wt.% Cu addition in Al alloy has also a much higher yield strength (YS) than Al alloy without Cu. However, the yield strength of the 1.0 wt.% Cu in Al alloy is a little lower than the alloy without Cu. Marioara et al [4] revealed, that the Cu-containing alloys (0.3 %Cu) achieve higher hardness due to finer microstructures with higher precipitate volume fractions as compared to their Cu-free counterparts. Moreover, Cu-containing alloys are less sensitive to Mg/Si ratio as compared to the Cu-free alloys. Płonka et al. [5] indicated, that the analysis of the EBSD structure and subgrain size measurements made on the extruded profiles have not revealed any significant differences between the alloy variants with 2.5% Cu and 3.5% Cu. Simultaneously, for variant 4.5% Cu, the structure is finer with the average subgrain size smaller by about 20% ($3.6 \div 3.9 \mu\text{m}$). However, the mechanical properties increase with the increasing Cu content in AlCuMgSiMn alloys. It should be noted that the addition of Cu can notably improve the strength of Al alloy, but it reduces its corrosion resistance. Wang et al. [6] revealed that the addition of Cu accelerates the immersion corrosion rate of Al alloy by 26.8% to 269.2%. This affects the peak ageing and overageing samples the most. The influence is less evident for underaged samples. At the same time, the addition of Cu reduces corrosion resistance by creating pitting at the first stage and intergranular corrosion around and inside the pitting hole.

On the other hand, for aluminium alloys, electron beam welding (EBW) is a very suitable process because the high-melting oxide film that interferes with other processes is easily destroyed by the movement of the electrons. Etching the workpiece surface in the weld area before welding reduces the oxide layer and thus improves the flow behaviour and weld quality with reduced porosity. The EBW of aluminium alloy as an autogenous (without filler material) or with filler material can be carried out. Furthermore, with EBW no problems arise from reflection of the beam resulting in reduced energy input. It is possible to achieve welding depths of 200 mm and more with good width to depth penetration ratio [7]. However, welding the aluminium alloys with electron beam process presents one problem specific to the process, that of metal vapour from the weld pool causing arcing inside the electron beam gun. This is a particular problem with those that contain low boiling point alloys such as magnesium and zinc. Arcing inside the gun interrupts the beam and causes cavities formation in the weld. Although some of the alloying elements, i.e. magnesium and zinc, are lost, this is generally insufficient to cause a loss of strength. Moreover, the use of these alloys is limited due to numerous other problems during fusion welding processes. One of the major problems with the fusion welding of this alloy is its high sensitivity to hot cracking [8], porosity [9] as well as excessive evaporation of light elements with high saturated vapor pressure [10]. The shrinkage due to solidification during EBW of the aluminium alloys is almost three times more than steel alloys [11], the weld metal in aluminium alloys undergoes a large dimensional change during the welding process leading to higher thermal induced stress and strain on the weld metal. Porosity supports the solidification cracking and acts as stress concentration sites resulting in a decrease in mechanical properties. The application of EBW with oscillation could be promising because of the smaller molten metal volume and longer time to diffuse hydrogen from the molten pool, along with perfect shielding of molten metal in a vacuum environment [9]. Thus, it is essential to find approaches to reduce the amount of porosity in welded joints and consequently elimination of cracks. Hosseini et al. [8] revealed that, higher welding speed and lower heat input led to decrease of the stresses and strains applied to the weld metal and therefore, the nucleation and growth of liquation hot cracking in the weld metal could be prevented. Moreover, the authors indicated that, simultaneous increase of welding power and welding speed resulted in the formation of the equiaxed dendritic microstructure in the bottom of weld metal. Thus, the propagation of hot cracks in this microstructure of weld metal is more difficult. They concluded that hot cracking can be eliminated in the specimens welded at speed of 30 mm/s and more. Sahul et al. [9] indicated that the utilization of beam oscillation resulted in the elimination of undercuts as well as porosity. Moreover, lowering the heat input resulted in the production of a smooth weld bead, with low amount of porosity. On the other hand, a larger beam current and a lower welding speed reduce the keyhole stability [12]. It should be noted that, due to the rapid cooling rate in the EBW molten pool, the ejected solute atoms during the solidification process have insufficient time to diffuse, resulting in an uneven element distribution and inevitable segregation. The segregation phenomenon may lead to uneven mechanical properties in the weld and even cracks, which are

detrimental to the final welded joint quality. Yang et al. [13] indicated that a keyhole is more stable when the inclination angle exceeds 90°, which means that the processing parameters with beam inclination angle greater than 90° is more inclined to prevent the formation of porosity defects in aluminium alloy. Kim et al. [14] indicated, that the weld strengths of square butt and U groove joints (AA6061-T6 alloy) were approximately 222 MPa (autogenous) and 247 MPa (with filler material). The joint efficiency of welded joint without filler was approximately 73% and the joint efficiency of welded joint with filler was 81%, respectively. It was found that the hardness variations of the filler metal addition exhibited higher hardness compared to the autogenous weld joint due to shear stresses induced by tool motion which led to the generation of a fine grain structure. Moreover, it was observed that the weld bead of U groove joint with filler wire was slightly wider than that of square butt joint. Alexopoulos et al. [15] revealed that heat treatment before as well as after welding influence of the mechanical properties of EB welded joints of 6156 aluminium alloy. Artificially ageing before the welding process results in the formation of Mg₂Si precipitates according to the different ageing condition. The EBW process allows dissolution all the formed precipitates within the fusion zone and enhance the ductility on the expense of strength properties of the welded joints. Over-ageing before welding gave the best results in tensile ductility properties. Ageing after the EBW process had the opposite effect between strength and ductility properties. Small ageing time is recommended (under-ageing condition) to increase the strength properties of the welded joint.

In this study, microhardness, microstructure, tensile and bend properties of AlSiMg(Cu) alloys in EBW was investigated. The influence of EBW technological parameters on properties of welded joints were discussed. SEM and EDS analysis studies were conducted to examine the effects of alloying elements as well as EBW parameters on the final properties. To the best of the authors' knowledge, this work is the very first attempt to apply EBW to a AlSiMg(Cu) aluminium alloys.

The main novelty of the presented results is the use of a new aluminium alloys with higher copper content, up to 1.4%. Currently, commonly used alloys in similar applications, such as the 6061 series, contain up to 0.4%. The addition of copper allows higher strengths achieved, but weldability is limited and susceptibility to hot cracking increased. To date, no attempts have been made to EB weld such alloys.

Experimental details

In this study, as-received AlSiMg(Cu) (without heat treatment) alloy flat bar with a dimension of 80×5 mm, were used. The chemical composition as well as mechanical properties of the samples are shown in Tables I and II, respectively. ARL 4460 optical emission spectrometer from Thermo Fisher Scientific for chemical analysis was applied. The sample surfaces were brushed and cleaned prior to testing. Measurements were taken at five different points. The average values are given in Table I. The mechanical tests acc. to EN ISO 6892-1 at room temperature were carried out. The tensile testing machine MTS Criterion C45 was applied.

Table I Chemical composition of the AlSiMg(Cu) alloys

Symbol	Element % wt.				
	Cu	Si	Mg	Mn	Others
1A	0.6	1.0	0.7	0.6	0.42
1B	0.8	1.0	0.7	0.6	0.42
2A	0.8	1.2	0.8	0.6	0.42
2B	1.0	1.2	0.8	0.6	0.42
2C	0.8	1.2	0.8	0.6	0.82
3A	1.2	1.2	0.8	0.6	0.57
3B	1.4	1.2	0.8	0.6	0.42

Table II Mechanical properties of the AlSiMg(Cu) alloys

Symbol	Mechanical properties ¹		
	Yield strength	Tensile strength	Elongation
	R _{0.2} MPa	R _m MPa	A ₅₀ %
1A	101.0 / 111.7	229.2 / 235.8	14.8 / 20.0
1B	108.0 / 99.7	245.1 / 234.8	19.6 / 14.8
2A	111.3 / 109.4	250.7 / 253.2	14.8 / 16.0

2B	112.4 / 118.7	255.8 / 264.9	15.6 / 16.2
2C	109.7 / 105.8	251.5 / 251.4	14.0 / 16.4
3A	143.0 / 135.2	308.9 / 298.2	13.0 / 12.2
3B	128.3 / 127.6	279.6 / 276.3	10.4 / 9.6

¹ Results for two specimens

This study, Cambridge Vacuum Engineering brand EBW model XW150:30/756 device for electron beam welding was used. Specimens 300×80×5 mm were welded together. The welding parameters are given in **Tab. III**. The pressure in the working chamber was below $5 \cdot 10^{-3}$ mbar. The beam axis of the EBW device was vertical, and all the welded joints were prepared in the flat position (1F/PA). The welding parameters were selected based on a preliminary study, and resulted in complete weld penetration, and a sound visual appearance and root formation. Before welding the plates were brushed as well as chemical cleaning with acetone. For final tests single welded joint for each of welding parameters were prepared. In

Table III EBW technological parameters

Parameter	Unit	Value
Acceleration Voltage, U	kV	80
Beam Current, I	mA	25.0 – 37.0 ¹
Welding Speed, v	mm/min	1000 / 2000 ²
Input Power, P	W	2000 – 2960 ¹
Input Energy, E	kJ/mm	0.023 – 0.038 ¹
Beam oscillation	-	Circle
Oscillation frequency, f	Hz	100
Oscillation amplitude	mm	1.0
Working distance	mm	470

¹ range of technological parameters, the min. and max. value. ² two welding speeds were applied

The quality of EB welded joints based on visual testing was controlled. EN ISO 17637 as well as standards EN ISO 13919-2 were applied. Moreover, the destructive tests were carried out. The tensile test specimens prepared acc. to EN ISO 4136 standard were subjected to a tensile test in MTS brand tensile testing machine (2 specimens for each set of parameters). The bend test with roller (4 specimens for each set of parameters) acc. to EN-ISO 5173 were conducted. The cross sections of welded joints were prepared for metallographic analysis by using standard metallographic procedure acc. to EN-ISO 17639. The welded joints specimens were etched by a modified Kroll's reagent. Metallographic analysis was conducted by using an Eclipse MA 200 (Nikon) light microscope. Hardness measurements were carried out in one line using a KB50 FA (Prüftechnik GmbH) hardness machine under a load of 1 kg (HV1, for 20 s) acc. to EN-ISO 22826. Microscopic observations in the cross-section of the welded joints were carried out. Inspect F-50 (FEI) scanning electron microscope (SEM) and energy-dispersive spectroscopy (EDS) and EDS mapping were used to characterize the microstructure of welded joints. The interface structure, and element distribution in the weld zone were analysed using a SEM equipped with an EDS analysis system.

Results

The EB butt welded joints were made with different combinations of welding parameters (see **Tab. III**) without filler materials (autogenous welding). Firstly, the lower welding speed (1000 mm/min) was applied at three different welding current. The increase of temperature of the welded plate, during welding, were considering. Thus, the lower welding current was used for second and third section of welded joint. Secondly, the higher welding speed (2000 mm/min) was used. The results of macroscopic examination of final welded joints are presented in **Fig. 1**. The quality of welded joints acc. to EN ISO 13919-2 was established. The main welding imperfection such as incompletely filled groove (511 acc. to EN ISO 6520-1) was detected. However, the dimensions of those imperfections are acceptable by the EN ISO 13919-2 standard. Acc to. EN ISO 13919-2 for a 5 mm thick plate at quality Level B the largest permissible incompletely filled groove defect is $\leq 0,5$ mm and for Level C ≤ 1 mm.

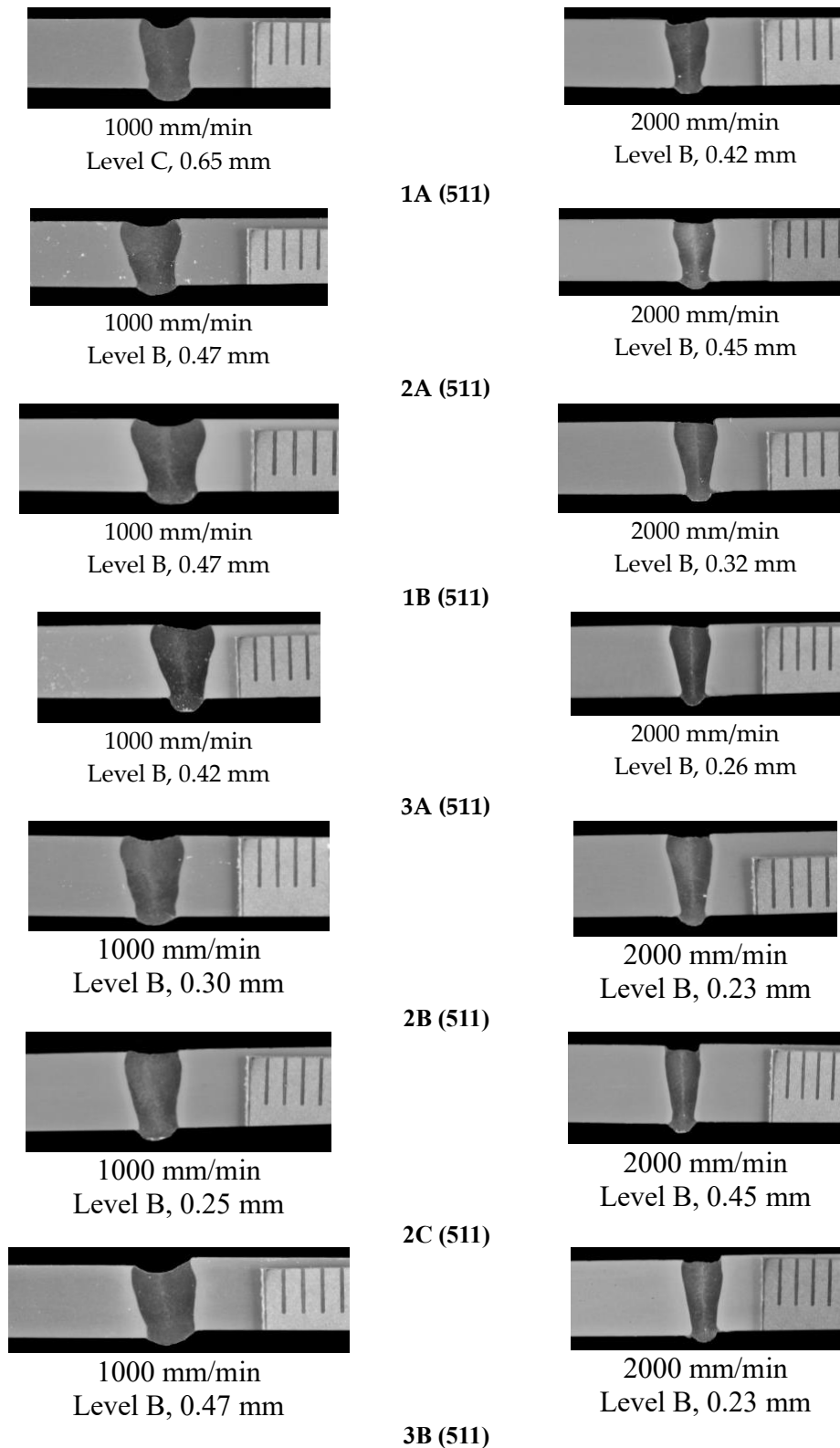
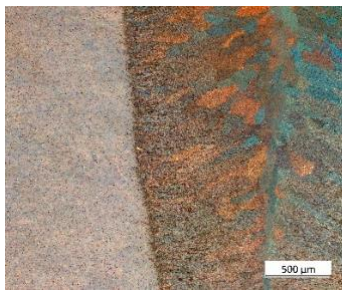
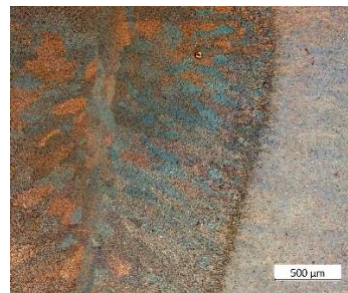


Fig. 1. Macroscopic examination, butt welded joints made with two different welding speeds, quality level acc. to EN ISO 13919-2, welding imperfections: incompletely filled groove (511), the results of measurements of imperfections were presented. Light microscopic examinations of the weld metal of all investigated alloys revealed a cellular dendritic structure with an equiaxed zone formation along the centreline of the weld as shown in Fig. 2 for 1A as well as 2A alloys (see Tab. I).



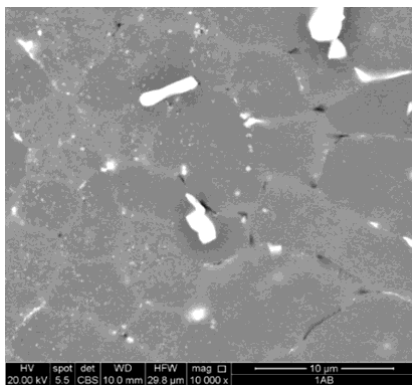
1A alloy



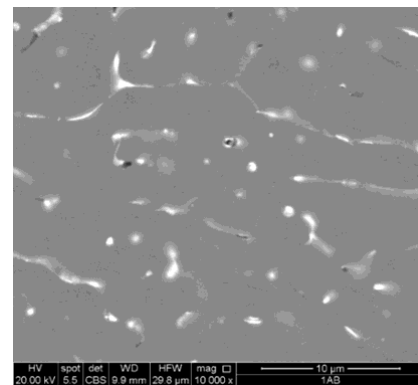
2A alloy

Fig. 2. Microscopic examination, butt welded joints of two Al alloys

SEM microscopic observations of welded joints revealed the influence of the EB welding on the morphology of the Mg₂Si phase. The growth and coagulation of this phase is visible in the heat affected zone (HAZ) area compared to the fusion zone (FZ). Moreover, a significant evolution of AlFeMnSiCu precipitates is also visible. The example results are presented in **Fig 3**. The images were formed backscattered electrons (SEM-CBS Concentric Backscattered Detector) technique.

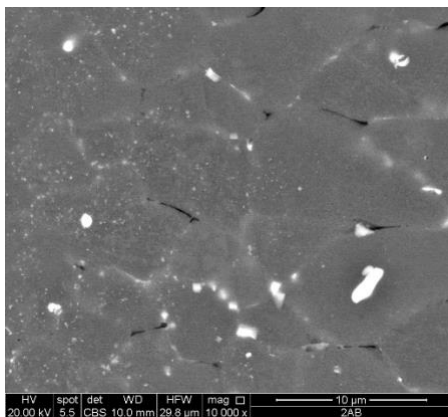


HAZ



fusion zone

Fig. 3. Microstructure of EB welded joint, 1A alloy, HAZ, SEM-CBS



HAZ

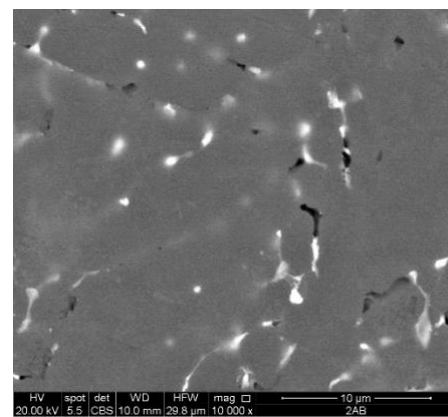


Fig. 3. Microstructure of EB welded joint, 2A alloy, HAZ, SEM-CBS

The analysis of the chemical composition in EDS micro-areas confirms occurring of different phases. Also using the EDS technique was proven that welding, apart the precipitations morphology changes, does not result in segregation of the chemical composition in individual areas of the joint. The results are presented in **Figs. 4** and **5**. However, more detailed analysis of the different phases in the welded joints of AlMgSi(Cu) alloy will be conducted in the future.

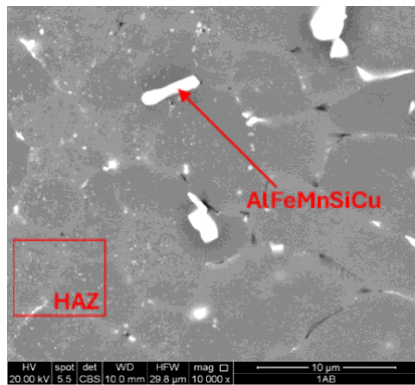


Fig. 4. Results of EDS analysis, 1A alloy, HAZ

Element	Chemical composition %wt.	
	HAZ	AlFeMnSiCu
Al	95.3	84.3
Mg	2.0	1.7
Si	1.0	5.1
Cr	0.4	1.0
Mn	0.7	5.5
Fe	-	1.8
Cu	0.6	0.5

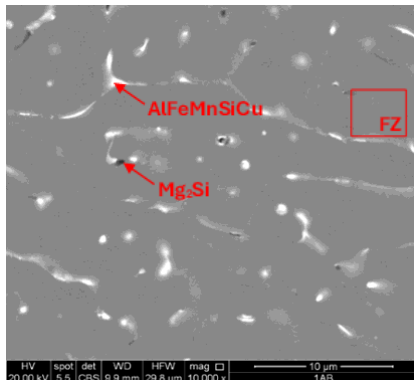


Fig. 5. Results of EDS analysis, 1A alloy, fusion zone

Element	Chemical composition %wt.	
	HAZ	AlFeMnSiCu
Al	95.9	87.4
Mg	1.9	1.9
Si	0.8	3.3
Cr	0.3	0.9
Mn	0.6	3.9
Fe	-	1.5
Cu	0.5	1.2

In order to characterise the mechanical properties of the butt-welded joints produced by EB welding process, hardness distribution as well as tensile and bend tests were performed. Fig. 6 and 7 shows example of hardness distribution on the welded joint cross sections. The applied load was 1 kg (HV1). The results also in Tab. IV were presented.

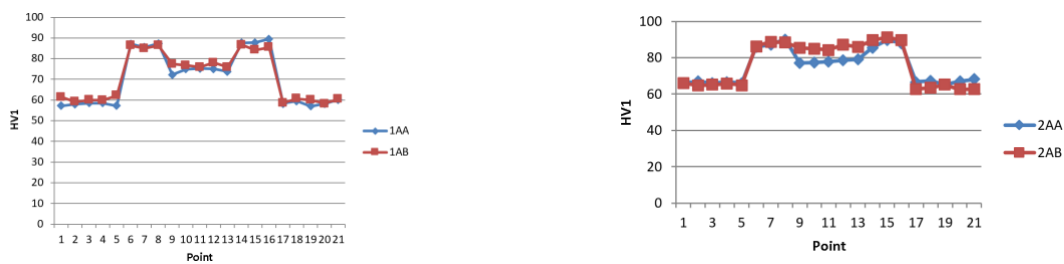


Fig. 6. Hardness distribution of welded joints (1A and 2A alloys), v=1000 mm/min specimens 1AA and 2AA, and v=2000 mm/min specimens 1AB and 2AB

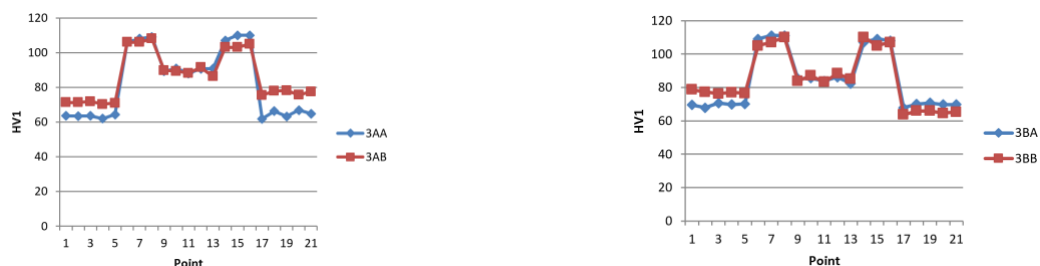


Fig. 7. Hardness distribution of welded joints (3A and 3B alloys), v=1000 mm/min specimens 1AA and 2AA, and v=2000 mm/min specimens 1AB and 2A

Table IV Results of hardness tests of EB welded joints

Area	Points																							
	Base material					HAZ					Weld					HAZ					Base material			
No	1	2	3	4	5	6	7	8	9	10	11	12	13	14	15	16	17	18	19	20	21			
1AA	57	58	59	59	57	87	86	87	72	75	75	75	74	88	88	90	58	60	57	58	60			
1AB	61	59	60	60	62	86	85	86	78	77	76	78	76	87	84	85	59	61	60	58	60			
2AA	66	67	66	67	66	86	87	90	77	77	78	79	79	86	90	88	67	67	65	67	68			
2AB	66	65	65	66	65	86	89	88	85	85	84	87	86	90	91	90	63	64	65	63	63			
3AA	64	63	64	62	64	106	108	109	89	91	88	91	91	107	110	110	62	66	63	67	65			
3AB	71	71	72	70	71	106	106	108	90	89	88	91	86	103	103	105	76	78	78	76	78			
3BA	69	68	71	70	70	109	111	111	85	85	84	86	82	107	109	108	68	70	71	70	70			
2BB	79	77	76	77	76	105	107	110	84	87	83	88	85	110	105	107	64	66	66	65	65			

The results of tensile tests for EB butt welded joints are presented in **Tab. V**. In comparison with mechanical properties of the base metal (BM), welding has resulted in deterioration of tensile strength of all the alloys investigated. However, **the strength retention was** about 81% for 3A alloys, and up to 99% 2A and 3B alloys. The samples, mainly, failed in the weld metal. Thus, the results are satisfactory. Acc. to ISO standard the efficiency of the welded joints must be higher than 60% [16]. However, for 2C the rupture in HAZ was also observed.

Table V Results of tensile test of EB welded joints

Symbol	Welding speed, mm/min	R_m , MPa	Remarks
1A	1000	225.9 / 211.6	rupture in weld
	2000	225.2 / 221.4	rupture in weld
$R_{m\text{ BM}}=232\text{ MPa}$	Joint efficiency %	91 ÷ 97	
1B	1000	238.8 / 231.6	rupture in weld
	2000	213.6 / 213.0	rupture in weld
$R_{m\text{ min BM}}=239\text{ MPa}$	Joint efficiency %	89 ÷ 99	
2A	1000	247.8 / 235.4	rupture in weld
	2000	231.6 / 228.8	rupture in weld
$R_{m\text{ min BM}}=256\text{ MPa}$	Joint efficiency %	91 ÷ 99	
2B	1000	236.4 / 238.4	rupture in weld
	2000	234.8 / 236.4	rupture in weld
$R_{m\text{ min BM}}=260\text{ MPa}$	Joint efficiency %	90 ÷ 92	
2C	1000	222.0 / 221.0	rupture in weld
	2000	220.7 / 224.0	rupture in HAZ
$R_{m\text{ min BM}}=251\text{ MPa}$	Joint efficiency %	88 ÷ 89	
3A	1000	244.1 / 249.1	rupture in weld
	2000	258.9 / 261.2	rupture in weld
$R_{m\text{ min BM}}=303\text{ MPa}$	Joint efficiency %	81 ÷ 86	
3B	1000	245.2 / 240.0	rupture in weld
	2000	274.3 / 275.7	rupture in weld
$R_{m\text{ min BM}}=277\text{ MPa}$	Joint efficiency %	87 ÷ 99	

However, the bend test with roller (angle up 180°) revealed that in the EB welded joints cracks occur (**Tab. VI**). Four specimens for each welding parameters were tested. The cracks up to 15 mm in lengths for some specimens were observed.

Table VI Results of bend test of EB welded joints

Symbol	Welding speed mm/min	Diameter of mandrel [mm]	Remarks
1A	1000	20	Without cracks
	2000		Without cracks
1B	1000	20	3 - without cracks, 1 - crack 15 mm
	2000		Without cracks
2A	1000	25	3 - without cracks, 1 - crack 5 mm
	2000		Without cracks
2B	1000	25	Without cracks
	2000		Without cracks
2C	1000	30	3 - without cracks, 1 - crack 5 mm
	2000		3 - without cracks, 1 - crack
3A	1000	30	3 - without cracks, 1 - crack 15 mm
	2000		3 - without cracks, 1 - crack 5 mm
3B	1000	40	3 - without cracks, 1 - crack 3.5 mm
	2000		2 - without cracks, 2 - cracks

Discussion

It can be observed based on macroscopic examination of EB welded joints (**Fig. 1**), that for lower welding speed the widths of the welds are visible greater. This is caused by the higher amount of energy (see **Tab. III**) compared to higher welding speed. Moreover, for lower welding speed the shape of the welds is less uniform than for high welding speed (parallel fusion lines). However, it should be noted, that for lower welding speed the porosity of welds can be reduced [17].

In general, that porosity formation is mainly attributed to insufficient surface cleaning of base metal prior to welding and insufficient shielding. Then, porosity level can be remarkably reduced by careful mechanical and chemical cleaning of base metal prior to welding and by vacuum. This means that the levels of porosity in the welds are dependent on the EB welding technology including welding parameters as well cleaning procedure. Both preweld surface cleaning and optimized parameters can be effective. Based on results of macroscopic examination of cross section of EB welded joints the porosity was not detected. However, it should be also noted, that for high welding speed, the solidification cracking problem can be observed [18]. These cracks are attributed to high stress concentration at the centre of weld bead due to its concavity and its high depth/width ratio because of unacceptable excess penetration. In our investigation, the solidification cracks were not observed in visual tests as well as macroscopic examination. It was also revealed, based on microscopic examination, that cracks were not observed along the boundaries of equiaxed zone formed along the weld centreline, and they were not confirmed to be solidification cracks. Generally, weld cracking in aluminium alloys can occur as a result of the aluminium relatively high thermal expansion, large change in volume upon solidification, and wide solidification temperature range. The investigated aluminium alloys with higher amount of Cu are known to be highly susceptible to weld cracks also in laser welding processes [18].

The microstructure in the weld, HAZ and initial material areas differs in terms of the distribution of fine-disperse phases inside the grains. In the tested materials (1A and 2B), a larger share of fine phases (β/Q) was observed outside the HAZ area. In the narrow HAZ zone, these phases were even finer, while in the weld, fine-disperse phases inside the grains were not observed. Due to the melting of the material, a characteristic dendritic structure was formed in the weld area (**Fig. 2**). Numerous elongated phases ($>1 \mu\text{m}$) were observed at the grain boundaries of the dendrites in the weld, rarely observed inside the grains. In the base material, due to the extrusion process, coagulated phases ($>2 \mu\text{m}$) were visible both inside the grains and at the boundaries. The conducted point chemical analyses (EDS) in micro-areas and based on the literature [19][20] show that these are phases of the following types: Q - AlSiMgCu, α - AlFeMnSiCu, β -Mg₂Si. Previous results indicated [18] that the precipitation sequence in AlMgSi(Cu) alloy is considerably more complex, and the precipitates are more numerous and varied depending upon the relative amounts of the different solutes present, including Cu. These alloys are strengthened primary by the β'' phase. Moreover,

the presence of L and Q' phase can be detected [20]. The L phase is different from Q' and occurs as a precursor to Q'. Phases Mg₂Si, AlFeMnSiCu, Q-AlSiMgCu in indicated areas of the welded joints can be also observed.

The hardness measurements clearly revealed, the higher hardness occurs in the HAZ. It should be noted, however, that for the EB welded joints six different alloys at different content of alloying elements (see Table I) were used. The results reveal that the hardness in the base material is much lower than in HAZ. Moreover, it can be observed that the hardness in fusion zone is slightly higher than in base material. Lower hardness value was found in HAZ as well as fusion zone for higher welding speed (2000 mm/s), and higher hardness value was found in FZ at 1000 mm/s (see **Tab. IV**, **Fig. 6** and **7**). The lower welding speed caused the higher cooling time. The total heat input (see **Tab. III**) is higher. Thus, more IMC is formed during welding at 1000 mm/min. As is known, Intermetallic compound (IMC) are hard structures [21]. El-Batahgy et al. [18] revealed that, the hardness of 6061 EB weld metal and HAZ was significantly increased by the postweld aging treatment, where it became close to that of the base metal. However, in the frame of presented research the mechanical properties as well as microstructure of samples as – welded were analysis.

Azadi and Kapranos [22] investigated the effects of EBW on microhardness and microstructural characterization of the 7075 aluminium alloy. Considering the microhardness values, it has been reported that the hardness of 130 HV in the BM increases up to 144 HV in the FZ. Balasubramanian et al. [23] examined the hardness changes of 7075 alloy in the TIG welding. They reported that the hardness, which was 136 HV in the BM, decreased in PMZ, and that it was at the lowest value (70–80 HV) in the FZ.

It should be noted that the hardness distribution corresponds with the microstructure of parts of welded joints and reflects their heterogeneity (see **Fig. 2-7**).

The properties of welded joints depend upon the chemical composition, the quality and the grain size of the deposit. These in their turn depend on the parent metal compositions (autogenous welding), the amount of dilution, the quality of the welding process and, lastly, the rate of solidification. Fast solidification rates will give a finer grain size and hence better mechanical properties than slow solidification rates (see **Tab. III**, **2C**, **3A** and **3B**). Small weld beads therefore generally have better properties than large weld beads and a higher resistance to hot cracking. However, in the root pass, a small cross-section weld bead may increase the risk as it will be required to carry the contractional stresses and restrain. This phenomenon is not observed in our results.

It can be noticed also that the lower strength in the weld metal can be accepted and compensated for in the design of final structures. It is clear that the post-weld aging treatment can be applied, and both tensile strength and elongation should increase to relation of the base metal. These improvements in the mechanical properties of postweld aged specimens are attributed to the reprecipitation of strengthening precipitates particles mainly of Mg₂Si in both weld metal and HAZ [18]. However, in our investigation the post-weld aging treatment was not applied. The welding process as well as all tests on the aluminium alloys as delivery conditions (delivery state F) were carried out.

The results confirm that the weldability as well as plasticity of AlSiMg(Cu) alloys is limited. All combined of tests allow to confirm the quality of final welded joints. The increase of Cu content cause increases the cracks sensitivity of alloys. The elongation alloys with high Cu content are limited up to 0.6% (see **Tab. I**). Therefore, during bend tests cracks can be observed.

Generally, to maintain the mechanical properties when welding aluminium alloys, the heat input and time of exposure to very high temperatures must be minimized. In comparison with arc welding processes, electron beam welding offers the benefits of low-heat input and extremely rapid cooling rate, all of which will help to minimize the metallurgical problems in the fusion zone. For example, high cooling rate will tend to slow down the development of blisters because of the short time in which the diffusion of hydrogen can take place. In addition, the low-heat input will tend to keep a very narrow HAZ then, retaining some to the strength of the material. Even though electron beam welding offers the advantages of a high energy density welding process, a vacuum chamber is required, which is not always practical [18].

Conclusions

In this study, an attempt to weld Al-Mg-Si alloys with higher content of Cu using EBW has been taken. This work aimed to check the possibility of joining a thermally unstable alloy with a simultaneous reduction of the heat input and avoiding excessive evaporation of the light elements with high vapor. From the conducted experiment, the following conclusions can be drawn:

- the use of high-power intensity focused electron beam with optimized parameters and careful material preparation prior to welding can produce welds with high quality. Porosity as well as cracks were not observed in the welded joints. However, the welding imperfection such as incompletely filled groove

and root concavity were detected. The level B and only for specimen 1A C level acc. to ISO 13919-2, were achieved.

- for both welding speed full penetration of 5 mm thickness welded joint was achieved. However, welding speed of 2000 mm/min have resulted in narrow width of welds for all alloys. Moreover, more parallel fusions lines are observed.
 - in the case of 6xxx alloys with the addition of Cu, the morphology of the phases plays a key role in the strengthening of the welded joint. The appearance of β and Q precipitates will additionally lead to the strengthening of the metal. A significant evolution of AlFeMnSiCu precipitates after welding is also visible.
 - in comparison with different alloys has experienced severe deterioration in mechanical properties due to softening in the fusion zone resulting from dissolution of the strengthening precipitates in the weld metal and HAZ. However, **the strength retention** was about 81-99% of base material. For example, the strength of the welded joint of 3B alloy was 275 MPa (base material 277 MPa). Thus, the max joint efficiency is 99%. However, the bend tests indicated that cracks up 3.5 mm occurred.

Author Contributions: conceptualization, M.W. and S.B.; methodology, B.P.; literature review, M.F. and K.F.; validation, M.W., and S.B.; formal analysis, M.W. and S.B.; investigation, M.M., P.S. and P.P.; resources, M.F., K.F.; data curation, M.M., J.H., P.S. and P.P.; writing—original draft preparation, M.W., S.B.; writing—review and editing, J.H., B.P; visualization, S.B., J.H., P.S; supervision, M.W. and B.P.; project administration, S.B.; funding acquisition, B.P.”.

Funding: This research was funded by The Polish National Centre for Research and Development, grant “Development of extrusion technology for sections from ultra-strength AlMgSi (Cu) alloys” number TECHMATSTRATEG-III/0040/2019”.

Conflicts of Interest: The authors declare no conflict of interest

References

- [1] L. Wang, M. Makhoulouf, and D. Apelian, “Aluminium die casting alloys: Alloy composition, microstructure, and properties-performance relationships,” *Int. Mater. Rev.*, vol. 40, no. 6, pp. 221–238, 1995, doi: 10.1179/imr.1995.40.6.221.
- [2] S. G. Shabestari and H. Moemeni, “Effect of copper and solidification conditions on the microstructure and mechanical properties of Al-Si-Mg alloys,” *J. Mater. Process. Technol.*, vol. 153–154, no. 10, pp. 193–198, 2004, doi: 10.1016/j.jmatprotec.2004.04.302.
- [3] Y. J. Li, S. Brusethaug, and A. Olsen, “Influence of Cu on the mechanical properties and precipitation behavior of AlSi7Mg0.5 alloy during aging treatment,” *Scr. Mater.*, vol. 54, no. 1, pp. 99–103, 2006, doi: 10.1016/j.scriptamat.2005.08.044.
- [4] C. D. Marioara *et al.*, “The effect of Cu on precipitation in Al-Mg-Si alloys,” *Philos. Mag.*, vol. 87, no. 23, pp. 3385–3413, 2007, doi: 10.1080/14786430701287377.
- [5] B. Płonka, K. Żyłka, K. Remsak, M. Rajda, J. Zdunek, and D. Moszczyńska, “Influence of copper content on the structure and properties of aluminium alloys,” *Arch. Civ. Mech. Eng.*, vol. 24, p. 8, 2024, doi: 10.1007/s43452-023-00811-7.
- [6] Z. Wang, L. Dong, B. Hu, and B. Chen, “The Effect of Cu Addition on Corrosion Resistance of Al-Si-Mg-Cr Alloy,” *Metals (Basel)*, vol. 13, no. 4, p. 795, 2023, doi: 10.3390/met13040795.
- [7] A. Volker, C. Uwe, D. Dietrich, T. Krussel, and T. Lower, “In Electron beam welding,” in *The fundamentals of a fascinating technology*, Gilching: Probeam AG&Co, 2011, pp. 30–31.
- [8] S. A. Hosseini, A. Abdollah-zadeh, H. Naffakh-Moosavy, and A. Mehri, “Elimination of hot cracking in the electron beam welding of AA2024-T351 by controlling the welding speed and heat input,” *J. Manuf. Process.*, vol. 46, pp. 147–158, 2019, doi: 10.1016/j.jmapro.2019.09.003.
- [9] M. Sahul, M. Sahul, M. Kritikos, and M. Vyskoč, “The effect of electron beam oscillation on the porosity of third-generation AW2099 aluminium lithium alloy welded joints,” *Mater. Lett.*, vol. 339, p. 134093, 2023, doi: 10.1016/j.matlet.2023.134093.
- [10] L. Zhao, S. Wang, Y. Jin, and Y. Chen, “Microstructural characterization and mechanical performance of Al-Cu-Li alloy electron beam welded joint,” *Aerosp. Sci. Technol.*, vol. 82–83, pp. 61–69, 2018, doi: 10.1016/j.ast.2018.08.030.
- [11] D. G. Eskin, Suyitno, J. F. Mooney, and L. Katgerman, “Contraction of aluminum alloys during and after solidification,” *Metall. Mater. Trans. A Phys. Metall. Mater. Sci.*, vol. 35, no. A(4), pp. 1325–1335, 2004, doi: 10.1007/s11661-004-0307-1.
- [12] Z. Yang, H. Fang, K. Jin, J. He, W. Ge, and W. Yan, “Modeling of microstructure evolution coupled with molten pool oscillation during electron beam welding of an Al-Cu alloy,” *Int. J. Heat Mass Transf.*, vol. 189, p. 122735, 2022, doi: 10.1016/j.ijheatmasstransfer.2022.122735.

- [13] Z. Yang and J. He, "Numerical investigation on fluid transport phenomena in electron beam welding of aluminum alloy: Effect of the focus position and incident beam angle on the molten pool behavior," *Int. J. Therm. Sci.*, vol. 164, p. 106914, 2021, doi: 10.1016/j.ijthermalsci.2021.106914.
- [14] S. Kim, Y. Jeong, J. Park, and Y. Lee, "Fundamental study on electron beam weld sections and strengths using AA6061-T6 aluminum alloy plate," *J. Mech. Sci. Technol.*, vol. 27, no. 10, pp. 2935–2940, 2013, doi: 10.1007/s12206-013-0806-3.
- [15] N. D. Alexopoulos, T. N. Examilioti, V. Stergiou, and S. K. Kourkoulis, "Tensile mechanical performance of electron-beam welded joints from aluminum alloy (Al-Mg-Si) 6156," *Procedia Struct. Integr.*, vol. 2, pp. 3539–3545, 2016, doi: 10.1016/j.prostr.2016.06.441.
- [16] "EN-ISO 15614-11 Specification and qualification of welding procedures for metallic materials Part 11: Electron and laser beam welding."
- [17] T. Yost and S. Liu, "Effects of select parameters on electron beam welding of AL6061-T6 alloy DOC. IV-1243-15.," *Mater. Sci. Eng. A*, vol. 459, no. 1–2, pp. 19–34, 2007, doi: 10.1016/j.msea.2006.12.125.
- [18] A. El-Batahgy and M. Kutsuna, "Laser beam welding of AA5052, AA5083, and AA6061 aluminum alloys," *Adv. Mater. Sci. Eng.*, p. 974182, 2009, doi: 10.1155/2009/974182.
- [19] D. J. Chakrabarti, Y. Peng, and D. E. Laughlin, "Precipitation in Al-Mg-Si alloys with Cu additions and the role of the Q' and related phases," *Mater. Sci. Forum*, vol. 396–402, no. (2), pp. 857–862, 2002, doi: 10.4028/www.scientific.net/msf.396-402.857.
- [20] L. Sagalowicz, G. Hug, D. Bechet, P. Sainfort, and G. Lapasset, "A study of the structural precipitation in the Al, Mg, Si system," in *4th International Conference on Aluminum Alloys*, 1994.
- [21] F. Hayat, "Electron beam welding of 7075 aluminum alloy: Microstructure and fracture properties," *Eng. Sci. Technol. an Int. J.*, vol. 34, p. 101093, 2022, doi: 10.1016/j.jestch.2022.101093.
- [22] A. A. Chegeni and P. Kapranos, "An experimental evaluation of electron beamwelded thixoformed 7075 aluminum alloy plate material," *Metals (Basel)*, vol. 7, no. 12, p. 569, 2017, doi: 10.3390/met7120569.
- [23] V. Balasubramanian, V. Ravisankar, and G. M. Reddy, "Effect of pulsed current and post weld aging treatment on tensile properties of argon arc welded high strength aluminium alloy," *Mater. Sci. Eng. A*, vol. 459, no. 1–2, pp. 19–34, 2007, doi: 10.1016/j.msea.2006.12.125.



Copyright: © 2026 by the authors. Licensee WTR, SIMP, Poland. This article is an open access article distributed under the terms and conditions of the Creative Commons Attribution (CC BY) license (<https://creativecommons.org/licenses/by/4.0/>).